

# The Effect of Heat Treatment on Mechanical Properties of Thermally Sprayed Sandwich Structure Beams

Saeid Salavati, Thomas W. Coyle, and Javad Mostaghimi

(Submitted March 22, 2015; in revised form August 21, 2015)

The application of metallic foam core sandwich structures in engineering components has been of particular interest in recent years because of their unique mechanical and thermal properties. Thermal spraying of the skin on the foam structure has recently been employed as a novel cost-efficient method for fabrication of these structures from refractory materials with complex shapes that could not otherwise be easily fabricated. The mechanical behavior of these structures under flexural loading is important in most applications. Previous studies have suggested that heat treatment of the thermally sprayed sandwich structures could improve the ductility of the skins and so affect the failure mode. In the present study, the mechanical behavior of sandwich beams prepared from arc sprayed alloy 625 skin on 40 ppi nickel foam was characterized under four point bending. The ductility of the arc sprayed alloy 625 coatings was improved after heat treatment at 1100 and 900 °C while the yield point was reduced. Heat treatment of the sandwich beams reduced the danger of catastrophic failure.

**Keywords** alloy 625, annealing, cracking, flexural test, four point bending, sandwich structure, twin wire arc spray

## 1. Introduction

Metallic foam core sandwich structures have been the focus of many manufacturers in recent decades because of their unique properties such as high surface to volume ratio, high strength to weight ratio, and also special physical properties (Ref 1-3).

Different fabrication methods, such as brazing of metal sheets, have been used to join the faces to the foam core to fabricate metallic foam core sandwich structures (Ref 1). These methods have limitations in shaping and joining of the skins, especially for complex structures (Ref 4). Thermal spraying of coatings on the foams to produce the skins has been introduced as a new method for production of these structures (Ref 3, 5, 6). Among thermal spray processes, twin wire arc spraying in air atmosphere was selected as a cost-efficient process that is capable of mass production of engineering components.

This article is an invited paper selected from presentations at the 2015 International Thermal Spray Conference, held May 11-14, 2015, in Long Beach, California, USA, and has been expanded from the original presentation.

**Saeid Salavati, Thomas W. Coyle, and Javad Mostaghimi**, Centre for Advanced Coating Technologies, 8th Floor, Bahen Building, 40 St. George Street, Toronto, ON M5S 3G8, Canada. Contact e-mail: salavati@mie.utoronto.ca.

The mechanical performance of the thermally sprayed metallic foam core sandwich structures is an important factor for engineering applications. The thermal spray coating deposited on the foam substrate is considered as structural element. The application of post-spraying heat treatment may improve the mechanical behavior of the sandwich structures by increasing the coating ductility and adhesion strength. This could result in reducing the danger of premature brittle failure in the skin (Ref 7, 8). The effect of heat treatment on the flexural rigidity of the sandwich structures is not as clear as its effect on the ductility and adhesion strength. The aim of this study was to investigate the changes in the mechanical behavior of the sandwich panels as a result of heat treatment. Optimization of the heat treatment process was discussed based on the obtained results.

## 2. Materials and Experiments

### 2.1 Fabrication of Sandwich Panels

Nickel foam sheets (Inco Special Products, Mississauga, ON, Canada), 10 mm thick, of 40 pores per inch (PPI) were used as the core material of the sandwich beams, see Fig. 1.

To avoid penetration of the micro-scale sprayed droplets into the foam pores, a temporary surface was formed on the foam sheet surfaces. An epoxy-based paste was prepared by mixing 60 volume percent of a thermoplastic resin (Acrodur 950 L, BASF, Mississauga, Ontario, Canada) and 40 volume percent of alloy 625 powder (AM-DRY 625+45 –90 µm, Catalog number DSMTS-0085.6, Oerlikon Metco., Westbury, NY, USA). The paste was spread on the foam and pushed into the surface pores to

make a 1 mm thick layer on the foam substrate. The filled foam was placed in the oven and heated for 2 h at each temperatures of: 70, 90, 110, 130, 150, and 190 °C gradually to cure the paste and convert the thermoplastic epoxy into thermoset. The surface of the nickel foam sheet was then machined to remove the extra layer of the paste on the foam surface that covered foam struts. After the foam struts are observed on the surface, the filled foam surface was grit blasted to get the foam struts exposed above the surface. An approximately 400 micrometer thick layer of alloy 625 (Ni 58%, Cr 20-23%, Mo 8-10%, Fe 5%, Nb 3-4%; Sulzer Metco Inc., Westbury, NY) was sprayed on both sides of the prepared foam substrate using a twin wire-arc spraying system (ValuArc, Sulzer Metco Inc., Westbury, NY). Due to exposure of the nickel foam strut tips from the surface, the deposited coating cannot be uniform in the thickness and shows micron scale fluctuations in the cross section. However, the average thickness was the same for all the coatings. Spray process parameters and their levels of the twin wire are listed in Table 1.

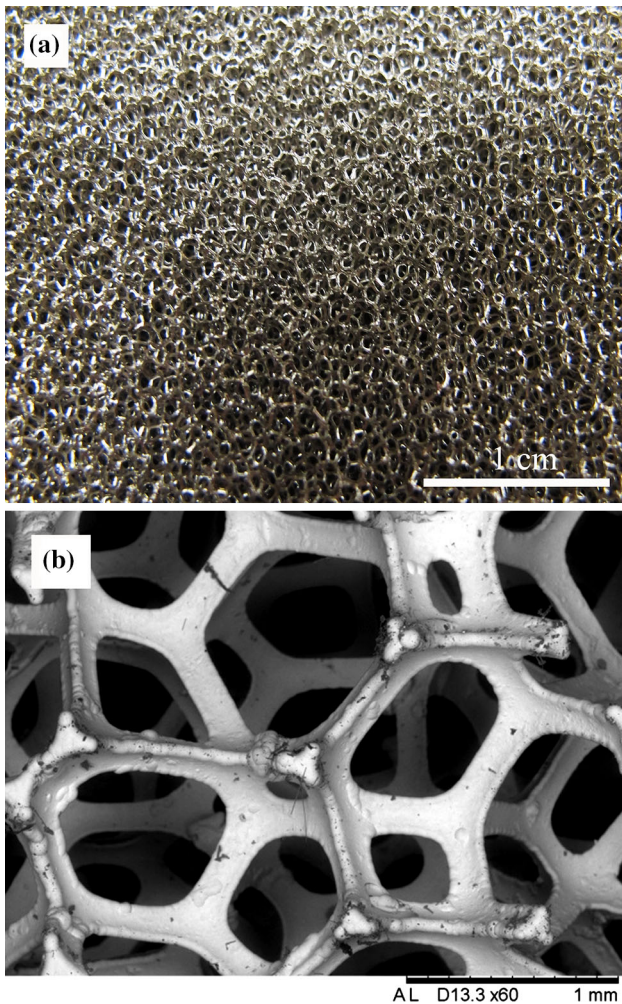


**Fig. 1** Nickel foam sheet (40 ppi) used as the sandwich core; (a) optical micrograph and (b) scanning electron micrograph (secondary electrons)

After deposition of alloy 625 coating on the sandblasted surface of the filled foam structures, sandwich panels were heated for 3 h at a temperature of 400 °C to degrade the epoxy part of the cured paste and burn out the binder. Then, the remaining metallic powder in the temporary surface was removed by shaking the panel.

Sandwich beams of 20 by 70 mm were cut out of the coated sheets for four point bending tests based on ASTM C 393 00 standard (Ref 9).

## 2.2 Heat Treatment

Samples with two replicates were heat treated at 1100 and 900 °C in a high-temperature vacuum furnace (Vac-Aero, Canada) for various dwell times, see Table 2. The heating and cooling rates were approximately 20°/min.

## 2.3 Microstructural Characterization

Microstructural observation of the coating and its interface with nickel foam was done by scanning electron microscopy (SEM) and energy dispersive x-ray spectroscopy (EDS) (TM3000, Hitachi High-Technologies Canada Incorporated, Toronto, ON). The porosity and oxide content of the coatings were calculated by employing an image analysis software, ImageJ (a Java-based image processing software developed at the National Institutes of Health in USA publicly available at <http://imagej.nih.gov/ij/>) (Ref 10). Image analysis (IA) is a reliable technique for quantification of the microstructural features in thermal spray coatings, with an uncertainty of approximately 2% (Ref 11, 12). In this research, coating cross sections were mounted and polished using an automatic polisher machine (EcoMet 250, Buehler, Whitby, ON, Canada). Secondary electron images were taken from the cross section of prepared samples for a better contrast between the splats cross section and the pores. Three main

**Table 1** Spraying parameters and their levels for production of alloy 625 coatings

| Parameter              | Value |
|------------------------|-------|
| Wire feed rate (m/min) | 7     |
| Voltage, V             | 34    |
| Current, A             | 298   |
| Inlet pressure, bar    | 5.8   |
| Air flow rate, slpm    | 1700  |
| Spraying distance, cm  | 10    |

**Table 2** Heat treatment temperatures and dwell times for sandwich beams

| Sample     | HT temperature, °C | HT dwell time, h |
|------------|--------------------|------------------|
| As-sprayed | N/A                | 0                |
| 900-1      | 900                | 1                |
| 900-3      | 900                | 3                |
| 900-5      | 900                | 5                |
| 1100-1     | 1100               | 1                |
| 1100-3     | 1100               | 3                |
| 1100-5     | 1100               | 5                |



phases were recognized in the alloy 625 coating: a metallic phase with lighter color, an oxide phase in gray and pores with darker color. This contrast differences enables for application of image analysis tools to calculate the quan-

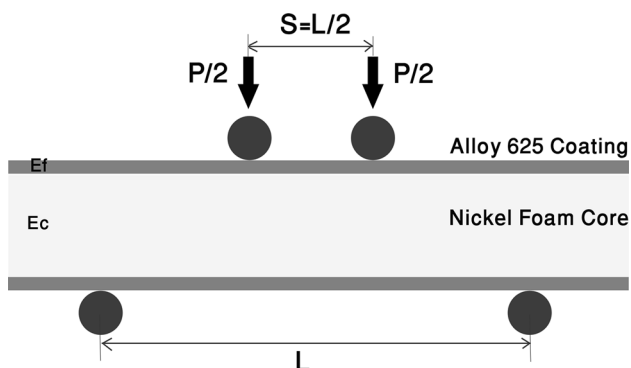


**Fig. 2** Schematic of foam core sandwich structure mounted in a four point bending test apparatus

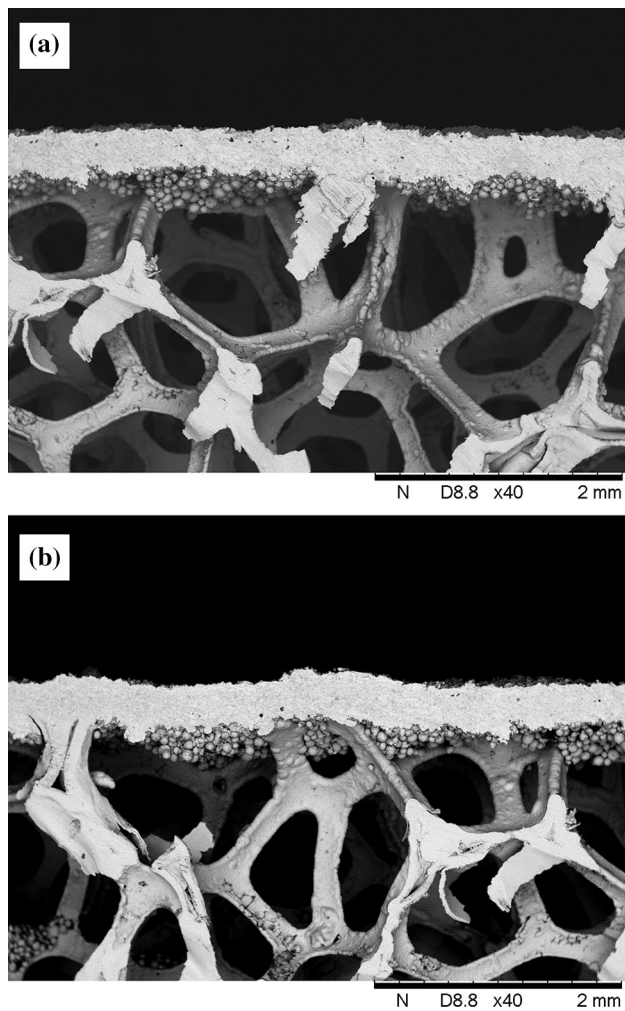


**Fig. 3** Cross section of 400  $\mu\text{m}$  thick alloy 625 coating deposited on foam substrate (a) as-sprayed (b) after 3 h annealing at 900  $^{\circ}\text{C}$

tity of each phase. The threshold was adjusted manually for accurate detection of the pores by comparing with the actual SEM images. The area of the black spots (pores) and the white matrix (metallic and oxide phases) was calculated and processed for quantification of the porosity content. Porosity measurement was conducted by analyzing at least ten SEM images taken from various spots for each sample. This procedure was also done for the calculation of the oxide content by changing the threshold and including the oxide phase in the black area.

The amount of the oxygen in the coating, as a factor of oxidation, resulted from EDS experiments on the coating cross section during SEM imaging.

#### 2.4 Four Point Bending Test

Four point bending is an appropriate technique for characterizing the rigidity and other aspects of the flexural behavior of sandwich beams (Ref 13-16), (Fig. 2). The rigidity ( $EI_{eq}$ ) can be determined from Eq 1 suggested by Azarmi et al. (Ref 14), which relates the center point deflection ( $\Delta$ ) to the applied load ( $P$ ) and flexural rigidity ( $EI_{eq}$ ):

$$\Delta = \frac{P(L-S)^2(L+2S)}{48EI_{eq}} + \frac{P(L-S)}{4U}, \quad (\text{Eq 1})$$

where  $U$  is the shear rigidity,  $S$  is the loading span,  $L$  is the support span, and  $P$  is the applied load.

The four point bending test apparatus was installed on a tension/compression testing machine (Autograph AG-I Universal tester, 50 KN, Shimadzu). The space between supporting rollers ( $L$ ) and loading rollers ( $S$ ) were 40 and 20 mm, respectively. During the experiment, the applied external force was recorded continuously while the crosshead moved at a constant rate of 2 mm/min. Each test was ended at the point of the first major load drop in the force-displacement diagram.

In the present study, sandwich panels with arc sprayed alloy 625 skins on nickel foam cores were fabricated, and

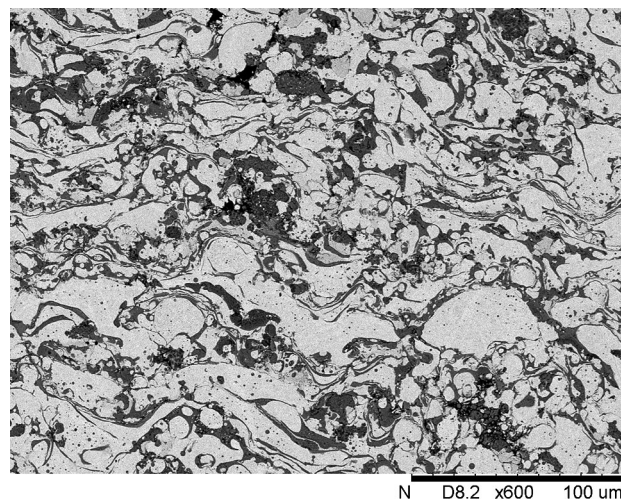
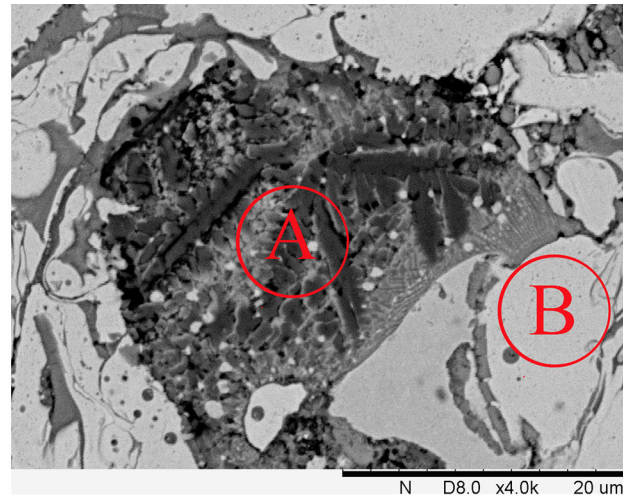


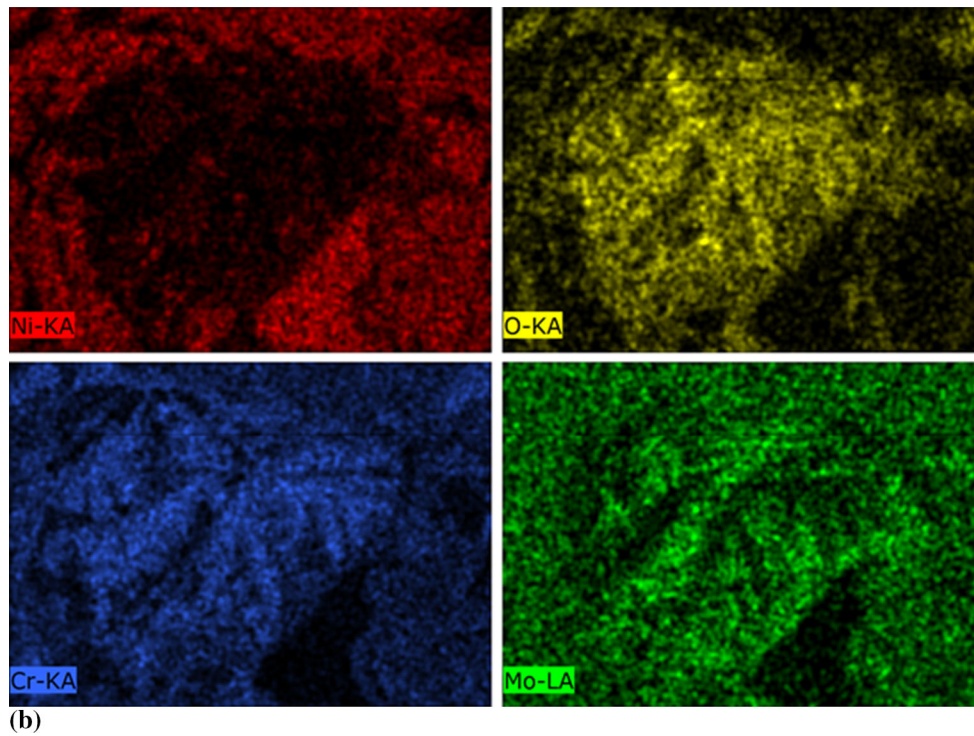
**Fig. 4** Microstructure of as-sprayed Inconel 625

then tested in four point bending as fabricated and after annealing at 1100 and 900 °C for 1, 3, and 5 h, respectively. Three samples were tested for each condition for

accuracy of the results. The effects of annealing process time and temperature on the flexural rigidity and the overall mechanical behavior were investigated.



(a)



(b)

**Fig. 5** (a) Microstructure of as-sprayed Inconel 625 in higher magnification (b)EDS map for Nickel, Molybdenum, Chromium, and Oxygen taken for the area shown in part a

**Table 3** Chemical composition of the phases present in the as-sprayed alloy 625 coating microstructure specified in Fig. 5

|        | Nickel, wt. % | Chromium wt. % | Molybdenum, wt. % | Oxygen, wt. % | Other elements, wt. % |
|--------|---------------|----------------|-------------------|---------------|-----------------------|
| Spot A | 16.67         | 34.34          | 8.93              | 29.19         | 10.87                 |
| Spot B | 53.54         | 19.92          | 10.04             | 1.23          | 15.27                 |



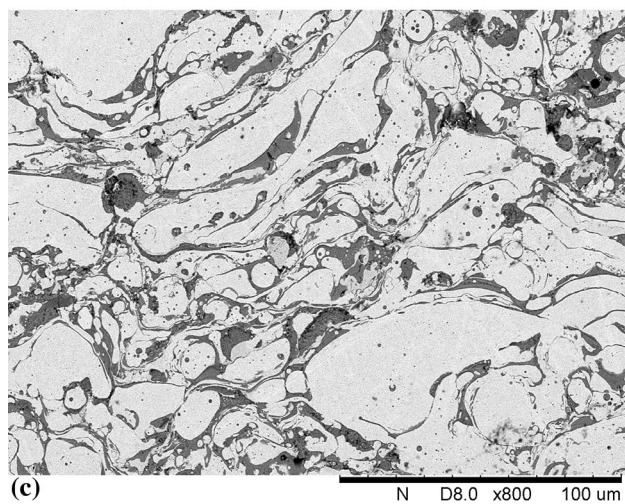
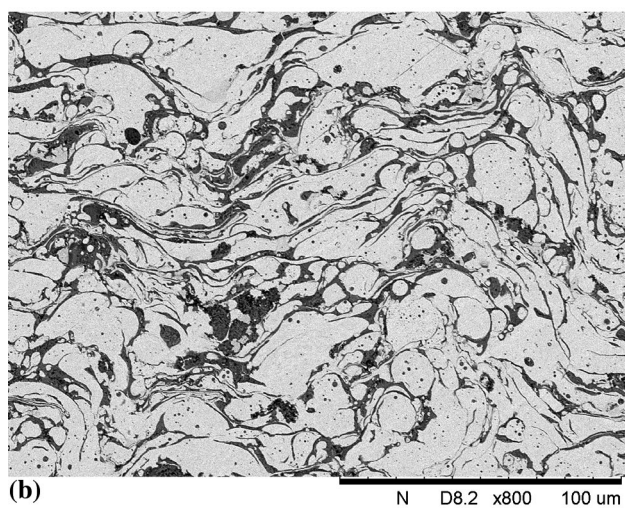
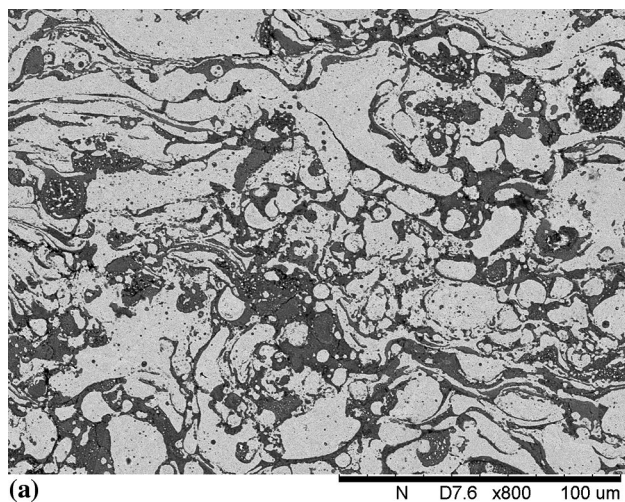


**Fig. 6** Microstructure of the alloy 625 arc sprayed coating after (a) 1 h annealing, (b) 3 h annealing, and (c) 5 h annealing at 900 °C

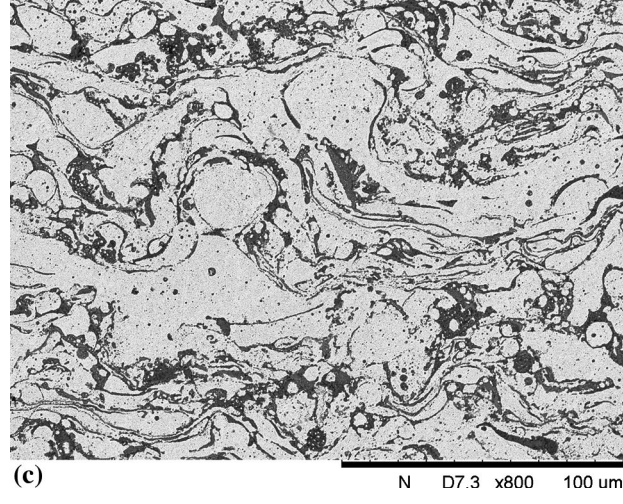
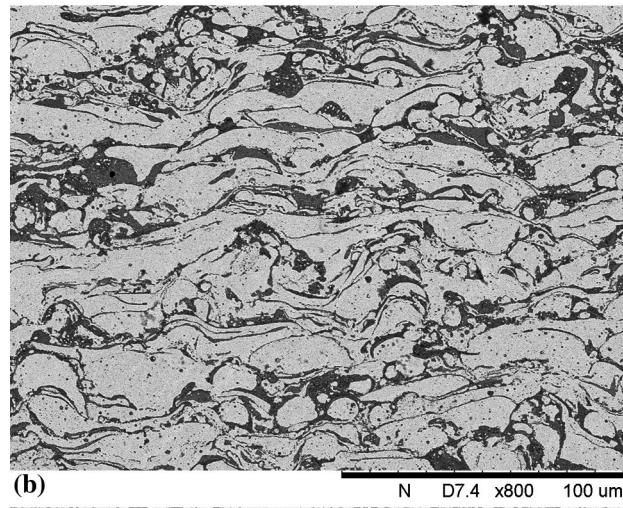
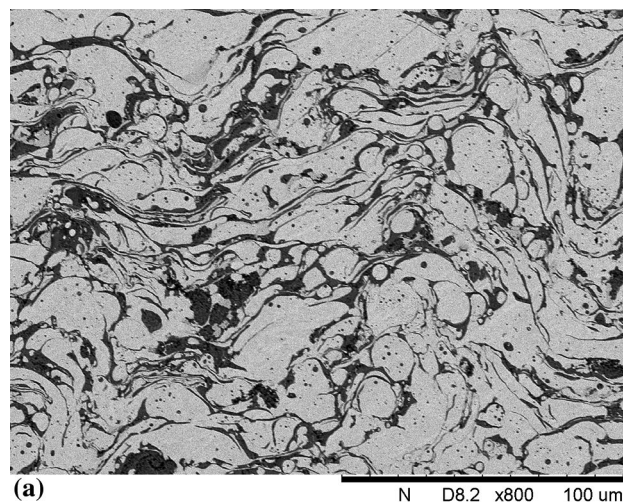


**Fig. 7** Microstructure of the alloy 625 arc sprayed coating after (a) 1 h annealing, (b) 3 h annealing, and (c) 5 h annealing at 1100 °C



### 3. Results and Discussion

#### 3.1 Microstructure of as-Sprayed and Annealed Coatings

Cross sections of the arc sprayed alloy 625 coatings on the foam substrate for as-sprayed sample and heat treated sample after 3 h annealing at 900 °C are shown in Fig. 3(a) and (b), respectively. It can be seen that the foam struts are embedded in the deposited coating and the temporary surface layer is not present in-between the struts and the coating. In fact, the application of grit blasting process before the coating deposition is to get the strut tips exposed from the temporary surface for mechanical bonding of the foam sheet to the skin.

It is commonly believed that annealing of thermally sprayed coatings leads to better connection between the individual splats in the coating and ultimately to better mechanical properties for the skin (Ref 17). Diffusion bonding across the splats may occur during the annealing process at high enough temperatures. This phenomenon leads to formation of metallurgical bonds between the splats, and improves the overall cohesive strength of the skin. Godoy et al. showed that the residual stresses stored in thermal spray coatings can be released by annealing, which eventually improves the mechanical properties of these coatings (Ref 18). The presence of pores in the

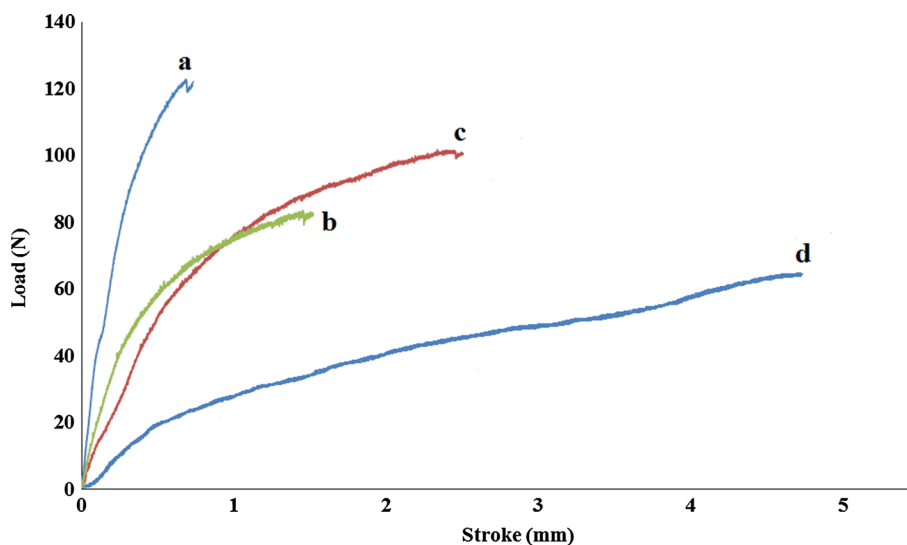
microstructure of the coating is also a significant factor in determining coating mechanical strength. Pores can act as stress concentrators that make crack formation and propagation easier inside the coating. It has been observed by Azarmi et al. that annealing can eliminate fine pores inside the coating microstructure and improves the mechanical properties (Ref 7). In addition to these findings, in this research, it was observed from the SEM images that the oxide content of the coating can be reduced by annealing the thermally sprayed coating in a vacuum furnace at high temperatures.

The SEM image of as-sprayed alloy 625 coating is shown in Fig. 4. It can be seen that a significant amount of the coating is formed by a dark phase distributed in-between a lighter color phase. Figure 5 shows the microstructure and EDS map of this dark phase in higher magnification along with the chemical composition of different color phases resulted from EDS spot test in Table 3. From the chemical compositions, it can be observed that the dark gray phase is mainly consisting of chromium and oxygen, while the light color phase is a nickel base alloy. This finding is proven in the EDS map that illustrates the higher concentration of oxygen and chromium in the gray phase. It can be concluded that chromium oxide is formed during spraying of alloy 625 and is finely distributed in-between the main metallic phase. Oxide phases are not desirable for engineering applications as they reduce the ductility of the coating due to the brittle nature of ceramic materials.

The microstructures of the alloy 625 coatings deposited on 40 ppi nickel foam annealed at 900 °C for 1, 3, and 5 h are shown in Fig. 6(a) to (c), respectively. Also, Fig. 7(a) to (c) show the microstructure of the alloy 625 coating annealed at 1100 °C for 1, 3, and 5 h, respectively. From the SEM images, it can be clearly seen that increasing the length of the annealing heat treatment results in a more uniform coating microstructure with less visible dark color

**Table 4** Porosity and oxide content of the skin

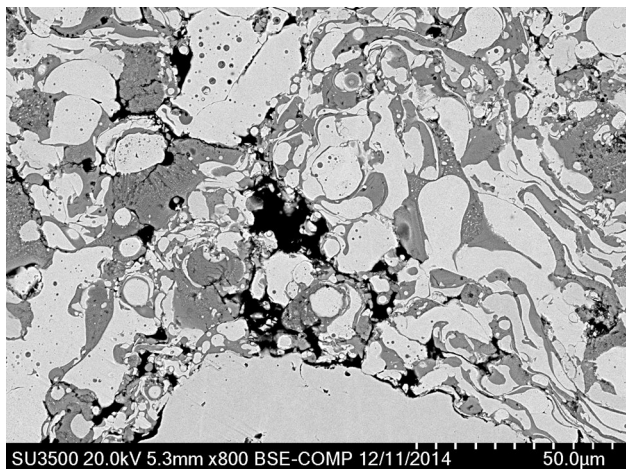
| Sample     | Porosity content, vol.% | Oxide content, vol.% |
|------------|-------------------------|----------------------|
| As-sprayed | 5 ± 1                   | 39 ± 5               |
| 900-1      | 5 ± 1                   | 36 ± 5               |
| 900-3      | 4 ± 1                   | 34 ± 5               |
| 900-5      | 3 ± 1                   | 31 ± 5               |
| 1100-1     | 4 ± 1                   | 32 ± 5               |
| 1100-3     | 3 ± 1                   | 28 ± 4               |
| 1100-5     | 2 ± 1                   | 25 ± 4               |



**Fig. 8** Typical force-displacement curves for (a) as-sprayed, (b) annealed for 3 h at 900 °C, (c) annealed for 3 h at 1100 °C, and (d) foam without coating

**Table 5 Flexural rigidity of the sandwich beams**

| Sample     | Flexural rigidity ( $EI_{eq}$ ), $N\ m^2$ |
|------------|---|
| Foam       | $0.05 \pm 0.01$                           |
| As-sprayed | $0.22 \pm 0.05$                           |
| 900-1      | $0.20 \pm 0.05$                           |
| 900-3      | $0.17 \pm 0.04$                           |
| 900-5      | $0.14 \pm 0.03$                           |
| 1100-1     | $0.18 \pm 0.04$                           |
| 1100-3     | $0.11 \pm 0.03$                           |
| 1100-5     | $0.09 \pm 0.02$                           |

**Fig. 9** Microstructure of the as-sprayed Inconel 625 skin close to the crack initiation region on the sandwich beam skin

oxide phase. Also, increasing the annealing time decreases the porosity content of the coating by eliminating more tiny pores. This effect was more significant for the samples annealed at 1100 °C than for the samples annealed at 900 °C. The porosity and oxide content calculated from SEM images by image J software for the samples annealed under different conditions are presented in Table 4.

### 3.2 Flexural Rigidity of the Sandwich Beams

The flexural rigidity,  $EI_{eq}$ , of the as-sprayed and annealed samples was calculated using Eq 1 and the initial portion of the force-displacement graph. The slope of the initial region in the force-displacement diagram yields the  $\frac{P}{\Delta}$  value for the linear (elastic) part of the behavior. The tension/compression machine crosshead displacement was taken as  $\Delta$ , the beam center point deflection.

Typical force-displacement graphs for the nickel foam without coating, as-sprayed sandwich panel, and 3 h annealed samples at 900 and 1100 °C are shown in Fig. 8. From the graphs, it can be seen that annealing of the sandwich beams reduces the yield point and the flexural modulus, but at the same time increases ductility. There-

fore, failure is initiated only after a significant threshold dislocation for the annealed sandwich structures.

The flexural rigidity was calculated based on the displacement of the crosshead movement. As the foam compression at the middle point of the sandwich structures was negligible, it can be claimed that the beam center point displacement is approximately the same as the cross head displacement. To calculate the flexural modulus of the samples, only the linear elastic range of the load-stroke diagrams that follows Young's behavior was used.

The experimentally determined flexural rigidity of the samples is shown in Table 5. The flexural rigidity of each sample has been reported as average values of replicates. It can be seen that the rigidity of the as-sprayed sample is higher than the annealed samples, but as was mentioned before, failure happened after very limited plastic deformation which may lead to catastrophic failure of this structure in engineering applications. Observation of the bending samples during the test showed that the initial failure happens on the edges of the lower skin in the middle of the beam length. This failure leads to a sharp drop in the load-stroke curve. To differentiate the foam failure due to compression from the skin cracking, the bending test was interrupted for several times during the test and the skins were carefully investigated. To gain a better understanding of the coating failure, the bending test was stopped right after observation of a tiny crack on the skin edge for an as-sprayed sample and it was cut along the crack line very carefully. The cross section was then prepared by minimum polishing and observed under SEM, see Fig 9. The resulting image shows cracks formed at the interface of the oxide phase and the metallic phase that could lead to separation of the coating parts and finally mechanical failure.

Based on the flexural rigidity calculations from the bending test results, it can be stated that by increasing the annealing time and temperature, the flexural rigidity is decreased. Therefore, an optimum heat treatment time and temperature should be sought in order to combine sufficient rigidity with a suitable ductility to avoid the danger of spontaneous skin cracking and catastrophic failure.

Figure 10 compares an as-sprayed beam with an annealed beam (3 h at 1100 °C) after failure. The crack on the surface of the as-sprayed sample (Fig. 10a) is evidence of a catastrophic failure because of low ductility of the as-sprayed thermal spray coatings. Annealing increases skin ductility, and thus, the plastic deformation of the sandwich panel before cracking, which eliminates catastrophic failure (Fig. 10b).

The four point bending test results showed that the annealing heat treatment procedure should be designed based on the application of the thermally sprayed metallic foam core sandwich structures in order to achieve an optimum ductility and flexural rigidity. In applications where deformation of the beam is negligible, annealing

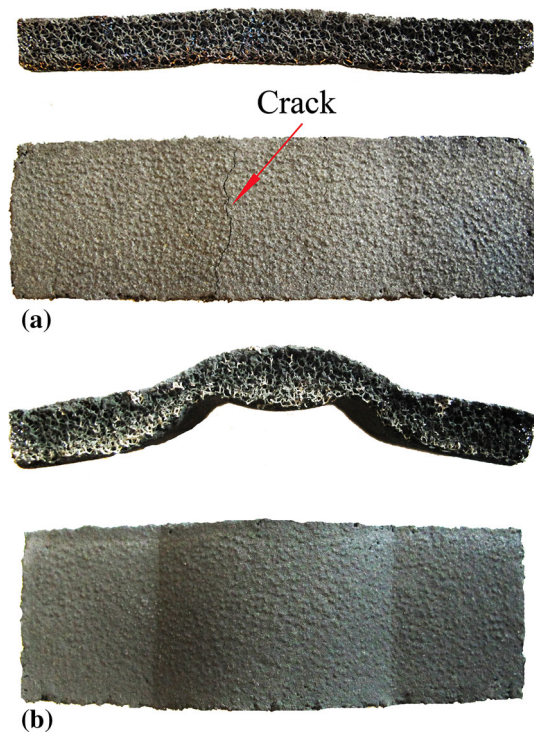


**Fig. 10** Arc sprayed foam core sandwich beams after four point bending tests (a) as-sprayed (b) annealed at 1100 °C for 3 h

can significantly improve the sandwich beam service life by reducing the cracking danger.

#### 4. Conclusion

Nickel foam core sandwich beams were fabricated by forming a temporary surface on both sides of nickel foam sheets, machining and sandblasting of the temporary surface and finally twin wire arc spraying of alloy 625 on the prepared substrate. Samples were annealed at 900 and 1100 °C to investigate the effect of heat treatment on the mechanical behavior of the sandwich beams. Four point bending tests were employed to experimentally determine the flexural rigidity of the sandwich beams. Results showed that heat treatment decreases the yield point and flexural rigidity of the beams, but improves the ductility of the skins, resulting in elimination of catastrophic failure by brittle cracking of the thermally sprayed skin layers. The optimum condition for high enough flexural rigidity and coating ductility must be chosen according to the sandwich beam application.

#### References

1. J. Banhart, Manufacture, Characterisation and Application of Cellular Metals and Metal Foams, *Prog. Mater. Sci.*, 2001, **46**(6), p 559-632
2. J. Banhart and W. Brinkers, Fatigue Behavior of Aluminum Foams, *J. Mater. Sci. Lett.*, 1999, **18**, p 617-619
3. H.R. Salimijazi, L. Pershin, T.W. Coyle, J. Mostaghimi, and S. Chandra, Metal Foam Sandwich Structure as a High Temperature Heat Exchanger, *2008 International Thermal Spray Conference & Exposition*, Vol. 1, 2008
4. H.R.S. Jazi, J. Mostaghimi, S. Chandra, L. Pershin, and T. Coyle, Spray-Formed, Metal-Foam Heat Exchangers for High Temperature Applications, *J. Therm. Sci. Eng. Appl.*, 2009, **1**(3), p 031008
5. F. Azarmi, J. Saaedi, T.W. Coyle, and J. Mostaghimi, Microstructure Characterization of Alloy 625 Deposited on Nickel Foam Using Air Plasma Spraying, *Adv. Eng. Mater.*, 2008, **10**(5), p 459-465
6. S. Salavati, R. Rezaey, L. Pershin, T.W. Coyle, and J. Mostaghimi, Development of High Density Twin Wire Arc Sprayed Coatings on Metallic Foam Substrates a b, *Proceedings of the International Thermal Spray Conference*, 2013, p 345-350
7. F. Azarmi, T. Coyle, and J. Mostaghimi, Young's Modulus Measurement and Study of the Relationship Between Mechanical Properties and Microstructure of Air Plasma Sprayed Alloy 625, *Surf. Coat. Technol.*, 2009, **203**(8), p 1045-1054
8. P. Callus and C. Berndt, Relationships Between the Mode II, Fracture Toughness and Microstructure of Thermal Spray Coatings, *Surf. Coat. Technol.*, 1999, **114**(2-3), p 114-128
9. ASTM international, Standard Test Method for Flexural Properties of Sandwich Constructions, *Annual Book of ASTM Standards*, ASTM international, 2000
10. S. Deshpande, A. Kulkarni, S. Sampath, and H. Herman, Application of Image Analysis for Characterization of Porosity in Thermal Spray Coatings and Correlation with Small Angle Neutron Scattering, *Surf. Coat. Technol.*, 2004, **187**(1), p 6-16
11. S.S. Madaeni, M.E. Aalami-Aleagha, and P. Daraei, Preparation and Characterization of Metallic Membrane Using Wire Arc Spraying, *J. Memb. Sci.*, 2008, **320**(1-2), p 541-548
12. A. Belenky and D. Rittel, Static and Dynamic Flexural Strength of 99.5% Alumina: Relation to Porosity, *Mech. Mater.*, 2012, **48**, p 43-55
13. K. Kanny and H. Mahfuz, Flexural Fatigue Characteristics of Sandwich Structures at Different Loading Frequencies, *Compos. Struct.*, 2005, **67**(4), p 403-410
14. F. Azarmi, T.W. Coyle, and J. Mostaghimi, Flexural Properties of Sandwich Beams Consisting of Air Plasma Sprayed Alloy 625 and Nickel Alloy Foam, *J. Mater. Sci.*, 2009, **44**(11), p 2836-2843
15. F. Azarmi, T.W. Coyle, and J. Mostaghimi, Evaluation of the Flexural Rigidity of Sandwich Structures Using Experimentally Obtained Mechanical Properties of the Constituents, *J. Therm. Spray Technol.*, 2009, **19**(1-2), p 429-438
16. M. Styles, P. Compston, and S. Kalyanasundaram, The effect of Core Thickness on the Flexural Behaviour of Aluminium Foam Sandwich Structures, *Compos. Struct.*, 2007, **80**(4), p 532-538
17. H.R.S. Jazi, T.W. Coyle, and J. Mostaghimi, Understanding Grain Growth and Pore Elimination in Vacuum-Plasma-Sprayed Titanium Alloy, *Metall. Mater. Trans. A*, 2007, **38**(3), p 476-484
18. C. Godoy, E.A. Souza, M.M. Lima, and J.C.A. Batista, Correlation Between Residual Stresses and Adhesion of Plasma Sprayed Coatings: Effects of a Post-annealing Treatment, *Thin Solid Films*, 2002, **420-421**, p 438-445